Rate Constant for the Reaction of OH with H_2 between 200 and 480 K†

Vladimir L. Orkin,* Sergey N. Kozlov,‡ Gregory A. Poskrebyshev,§ and Michael J. Kurylo||

Physical and Chemical Properties Division, National Institute of Standards and Technology, Gaithersburg, Maryland 20899

Received: December 2, 2005; In Final Form: March 2, 2006

The rate constant for the reaction of OH radicals with molecular hydrogen was measured using the flash photolysis resonance-fluorescence technique over the temperature range of 200−479 K. The Arrhenius plot was found to exhibit a noticeable curvature. Careful examination of all possible systematic uncertainties indicates that this curvature is not due to experimental artifacts. The rate constant can be represented by the following expressions over the indicated temperature intervals: $k_{H_2}(250-479\ \mathrm{K}) = 4.27 \times 10^{-13} \times (T/298)^{2.406} \times \exp\{-1240/T\}$ cm^3 molecule^{-1} s^{-1} above $T = 250$ K and $k_{H_2}(200-250\ \mathrm{K}) = 9.01 \times 10^{-13} \times \exp\{-(1526 \pm 70)/T\}$ cm^3 molecule^{-1} s^{-1} below $T = 250$ K. No single Arrhenius expression can adequately represent the rate constant over the entire temperature range within the experimental uncertainties of the measurements. The overall uncertainty factor was estimated to be $f_{H_2}(T) = 1.04 \times \exp\{50 \times |(1/T) - (1/298)|\}$. These measurements indicate an underestimation of the rate constant at lower atmospheric temperatures by the present recommendations. The global atmospheric lifetime of H_2 due to its reaction with OH was estimated to be 10 years.

Introduction

The simplest of OH reactions

$$\mathrm{OH} + \mathrm{H_2} \xrightarrow{k_{H_2}} \mathrm{H_2O} + \mathrm{H} \qquad (1)$$

plays a significant role in the chemistry of the Earth's atmosphere by converting OH to HO_2 (through the subsequent reaction of hydrogen atom with O_2). Because of the relatively large abundance of H_2 in the atmosphere, reaction 1 is important in evaluating the concentration of hydroxyl radicals. Molecular hydrogen is produced mainly via the oxidation of methane and nonmethane hydrocarbons (NMHCs) as well as from the combustion of fossil fuels and biomass.[1] Because of these sources, the budget of H_2 is tied to the cycling of CH_4, NMHCs, and CO via formaldehyde photolysis (which is the major immediate photochemical source of H_2 in the atmosphere). H_2 is removed from the troposphere by reaction 1 with OH as well as by soil uptake.

Thus, accurate information on the rate of reaction 1 under various atmospheric conditions is important in quantifying the H_2 budget and, thereby, the budgets of other coupled atmospheric species, including OH. The increasing interest in the possible buildup of a hydrogen fuel economy has led to suggestions that the H_2 atmospheric concentration could exceed its present value (ca. 0.53 ppmv[1]) substantially, increasing to greater than 2 ppmv because of unavoidable leakage of hydrogen into the atmosphere.[2] The change in the concentration of the major tropospheric oxidizer, OH, can be the most significant potential impact of such emission.[3] A reduction in the atmospheric concentration of OH will increase the residence time in the atmosphere for the majority of industrial and natural pollutants, which may cause related environmental feedbacks. Thus, the need to evaluate the total atmospheric impact of significant emissions of hydrogen[4,5] raises the importance of uncertainties in the rate constant of reaction 1.

Most studies of reaction 1 have been motivated by its role as a key reaction in H_2 combustion systems, and some of them have been conducted at exceptionally high temperatures (approaching 2500 K). However, the majority of direct determinations of the reaction rate constant have been performed at ambient temperature and over a limited temperature range. There have been only three laboratory investigations performed in the (below room temperature) region of atmospheric interest[6−8] that have provided a basis for quantifying the role of reaction 1 in the Earth's atmosphere. Unfortunately, these studies have not provided reliable direct measurements of the rate constant at temperatures below ca. 240 K and the currently available recommendations for atmospheric modeling community[9,10] are based mainly on simple extrapolation of near room-temperature experimental results to the region of atmospheric interest.

Reaction 1 is a benchmark system for the accurate theoretical investigation of reaction processes because it plays the same role in four-atom systems as H + H_2 plays in three atom systems. A number of modern theoretical approaches have been used recently to investigate the dynamics of the reaction and predict the kinetic reaction rate constant (refs 11−15 and references therein). Hence, accurate experimental data are needed to validate the results of such calculations, especially at lower temperatures where tunneling should play a significant role for this reaction.

Our own initial interest in this reaction stemmed from its kinetic and experimental simplicity, which might serve to "benchmark" our low-temperature kinetic measurement capability, thereby establishing the lack of experimental artifacts in our low-temperature flash photolysis resonance fluorescence investigations of the OH reactivity of hydrocarbons and halogenated hydrocarbons. Similarly, this simple OH reaction

† Part of the special issue "David M. Golden Festschrift".

‡ Present address: Institute of Biochemical Physics, Russian Academy of Sciences, Moscow, 117997, Russia.

§ Present address: Oak Crest Institute of Science, 2275 E. Foothill Blvd., Pasadena, CA 91107.

|| Present address: Science Mission Directorate, National Aeronautics and Space Administration, Washington, D.C. 20546.

10.1021/jp057035b CCC: $33.50
Published on Web 04/22/2006

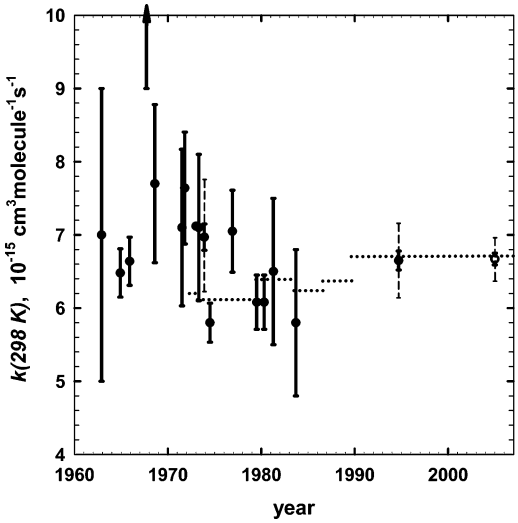

Figure 1. Reported results of the reaction rate constant measurements at $T = 298$ K, $k_{H_2}(298\ K)$ with associated statistical (bold error bars) and estimated systematic (dashed error bars) uncertainties (refs 6−8 and 16−28). The open circle is the result of this investigation. The dotted horizontal lines represent the evolution of $k_{H_2}(298\ K)$ recommended by the NASA Data Evaluation Panel for atmospheric modeling.

could serve as a "standard" to calibrate new experimental efforts in OH reactivity measurements. However, it became obvious immediately that the rate constant of this intensively studied reaction still has fairly large uncertainty, particularly at lower temperatures. Sixteen investigations[6−8,16−28] of this reaction at and around room temperature have been performed since the first experimental study by Kaufman and Del Greco in 1963.[16] In Figure 1 we summarize all of the available experimental results obtained for the rate constant of this reaction at $T =$ 298 K with the originally reported uncertainty bars along with $k_{H_2}(298\ K)$ recommendations given by the NASA Panel for Data Evaluation (horizontal dotted lines).

The majority of the previous publications reported reasonably consistent average values for the room-temperature rate constant, $k_{H_2}(298\ K)$, which are within ca. 10% of the currently recommended one. This agreement formed the basis for the current recommendation of $k_{H_2}(298\ K)$ well before the most recent and precise study of this reaction.[8] Unfortunately, reported statistical uncertainties (shown in Figure 1) were too large to allow a narrowing the uncertainty limits of the recommendation, even at the room temperature, and any estimated systematic errors make this situation even worse.

In this paper we report results of intensive study of the title reaction, which was concentrated on lowering the uncertainty of the rate constant at room temperature and below and providing the experimental data at lower temperatures of atmospheric interest.

Experimental Section[29]

Detailed descriptions of the apparatus and the experimental method used to measure the OH reaction rate constants are given in previous papers.[30−32] The principal component of the flash photolysis-resonance fluorescence apparatus is a Pyrex reactor (of approximately 50 cm^3 internal volume) thermostated with methanol, water, or mineral oil circulated through its outer jacket. The reaction 1 was studied in argon carrier gas (99.9995% purity) at a total pressure of 2.20−13.33 kPa (16.5−100.0 Torr). Helium (99.999%) was used as the carrier gas instead of argon in a few test experiments. Flows of dry argon, argon bubbled through water thermostated at 276 K, and hydrogen mixtures (containing 2%, 10%, and 50% of H_2) diluted with argon were premixed and flowed through the reactor at a total flow rate between 0.24 and 1.4 $cm^3\ s^{-1}$, STP. The concentrations of the gases in the reactor were determined by measuring the mass flow rates and the total pressure with a MKS Baratron manometer. Flow rates of argon, the H_2O/argon mixture, the N_2O/argon mixture, and the H_2/argon mixture were measured using Tylan mass flow meters directly calibrated for each mixture. A 50% mixture of H_2 in argon instead of pure hydrogen was used to measure the smallest reaction rate constants at low temperatures because of the more stable operation of mass flow meters, thus resulting in smaller uncertainty in the H_2 concentration.

Hydroxyl radicals were produced by the pulsed photolysis (0.15−3 Hz repetition rate) of the precursor by a xenon flash lamp focused into the reactor. The majority of measurements were performed by using the photolysis of H_2O, injected via the 276 K argon/water bubbler. (This argon/water bubbler was maintained at $T = 293$ K in some test experiments to further increase the concentration of H_2O in the reactor.) The use of the below room-temperature water bubbler ensures the smaller and more stable concentration of water vapor in the reactor. The lowest temperature for measurements using H_2O as the precursor was 215 K. The photolysis of N_2O producing $O(^1D)$ followed by its reaction with H_2 was employed as the OH source to study the reaction at $T = 200$ K. The consistency of results obtained with two different sources of OH was checked at $T =$ 250 K and $T = 215$ K. The OH radicals were monitored by their resonance fluorescence near 308 nm, excited by a microwave-discharge resonance lamp (330 Pa or 2.5 Torr of a ca. 2% mixture of H_2O in UHP helium) focused into the reactor center. The resonance fluorescence signal was recorded on a computer-based multichannel scanner (channel width 100 μs) as a summation of 300 to 5000 consecutive flashes. The resonance fluorescence decay at each reactant concentration was analyzed as described by Orkin et al.[31] to obtain the first-order decay rate coefficient due to the reaction under study.

The molecular hydrogen concentration ranged from ca. 2×10^{14} to 2×10^{17} molecules/cm^3. At each temperature the rate constant was determined from the slope of a plot of the decay rate versus molecular hydrogen concentration. The [OH] decay rate due to the reaction with H_2 ranged from ca. 8 s^{-1} to ca. 320 s^{-1} in our experiments. The temperature points for the measurements were chosen to be approximately equally distant along the Arrhenius $1/T$ scale (except the lowest temperatures) in order to have them properly, that is, equally, weighted in the following fitting procedure. In particular, experiments were performed at the two temperatures that are used widely in other studies, $T = 298$ K and $T = 272$ K. The first one is the standard temperature used in the evaluations and presentations of the rate constants while the second one is the temperature used in estimations of the atmospheric lifetime[33] (see eq 21 below). To check for any complications, test experiments were performed with the following variations of experimental parameters: the total pressure in the reactor (a factor of 6, between 16.5 and 100 Torr), the precursor, H_2O concentration (a factor of 150), the flash energy (a factor of 8), the flash repetition rate (a factor of 20, between 0.15 and 3 Hz), and the residence time of the mixture in the reactor (a factor of 3).

Uncertainties due to systematic effects in our measurements can be associated with such procedures as the absolute calibration of the MKS Baratron manometer (which measures the pressure in the reaction cell), the calibrations of the three Tylan mass flow meters (argon, argon/water, and H_2/Ar flows), and the temperature stability and measurements in the reaction cell.

The stated accuracy of the reaction cell manometer (ca. 0.1%) was verified by its absolute calibration. The two MKS Baratron manometers, 100 Torr (13.33 kPa) and 1000 Torr (133.3 kPa), used to prepare the H_2/Ar mixtures were intercalibrated and their linearity was found to be accurate to within ca. 0.2%. The H_2/Ar mixtures containing 2.00%, 10.0%, and 50.0% H_2 in argon were prepared in 5 L glass bulbs with the attention paid to their thermal equilibration. In our previous studies we also verified the concentration of manometrically prepared reactant mixtures using UV absorption measurements to find no discrepancy within the accuracy of absorption measurements of halogenated hydrocarbons. We do not expect any uncertainty due to adsorption/desorption of such a volatile gas as molecular hydrogen. All mass flow meters were calibrated for the appropriate mixtures by measuring the rate of pressure change in the same reaction cell (an additional volume was connected for larger flow rates) isolated from the vacuum pump by using the same reaction cell manometer. These calibrations were usually reproducible within 0.5−1%. The determination of the reactant concentration in the reactor requires only relative gas flow rates and one absolute pressure measurement. Therefore, this calibration procedure allows us to minimize the related instrumental uncertainty of the measurements. The uncertainty of the gas temperature in the reactor was less than 0.3 K between 250 and 370 K. This increased up to 1 K at the low-temperature end and to about 2 K at the high-temperature end of the temperature range used in this study due primarily to temperature fluctuations during the multiflash experiment. The relative error that can be introduced by the gas temperature fluctuations is offset to some extent by the opposite temperature dependencies of the reactant concentration and the measured rate constant.[34] To quantify the combined uncertainty associated with our experimental procedure, we added the square root of the sum-of-the-squares of the flow meter calibration uncertainties to the other uncertainties mentioned above. Thus, we estimate the expanded uncertainty due to possible instrumental effects to be ca. 3% increasing up to 6% at the lowest temperatures.

All of the experiments were performed with "research grade" hydrogen from Spectra Gases Inc. (99.9999% stated purity with less than 0.1 ppm stated level total halocarbons impurity). A few test experiments were performed with "prepurified" grade hydrogen from Matheson (99.99% stated purity with less than ca. 0.8 ppm of total halocarbons impurity). The N_2O sample had the manufacturer's stated purity of 99.9+%.

Results and Discussion

The rate constants obtained for the title reaction at various temperatures are presented in Table 1 along with information on the reactant concentration ranges and number of experimental determinations (number of measured decays rates) associated with the final values at each temperature. These data are shown in Figure 2. The bold highlighted data at each temperature were then used to derive the temperature dependence of the rate constant. The reported statistical uncertainties always represent two standard errors from the fit to the data points. The total uncertainties (in parentheses) are the statistical two standard errors plus the estimated systematic uncertainties derived above.

Kinetic Measurements: H_2O and N_2O Photolysis Experiments. The values reported in Table 1 were obtained in the experiments performed at 30 Torr (4.0 kPa) total pressure with H_2O photolysis as the OH source between 215 and 479 K. On the basis of the high precision and reproducibility of the data we were able to do numerous test experiments with variation of different parameters to check and/or avoid any sources of systematic errors. Some of the reported values were derived from the fit to the experimental points obtained over a long period of time, using independent calibrations. Therefore, even the reported statistical error may actually incorporate some systematic uncertainties.

TABLE 1: Results of the Rate Constant Measurements for the Reaction between OH and H_2[a]

T, K	$k_{H_2}(T)$, 10^{-15} cm^3 molecule^{-1} s^{-1}	H_2 concentration range, 10^{16} molecule/cm^3	(number of points)
479	**100.8 ± 2.7** (7.0)	0.028 − 0.31	(19)
419	**49.54 ± 0.73** (2.80)	0.032 − 0.36	(26)
370	**25.8 ± 0.68** (1.70)	0.072 − 0.78	(25)
330	**12.66 ± 0.44** (0.89)	0.40 − 1.4	(7)
298	**6.67 ± 0.08** (0.25)	0.17 − 2.4	(116)
272	**3.55 ± 0.088** (0.21)	1.29 − 8.82	(24)
250	**1.98 ± 0.053** (0.13)	1.2 − 8.8	(31)
	1.97 ± 0.093	1.4 − 7.1	(11)
230	**1.185 ± 0.04** (0.095)	0.8 − 8.7	(79)
220	**0.910 ± 0.037** (0.084)	1.5 − 7.9	(21)
215	0.785 ± 0.038	*0.8 − 4.9*	(*40*)
	0.740 ± 0.034 *(0.078)*	1.6 − 10.5	(7)
200	***0.43 ± 0.03*** *(0.056)*	2.5 − 15.5	(48)

[a] Uncertainties represent statistical two standard errors from the fit (values in parentheses include estimated systematic uncertainties). The reaction rate constants derived in this study at each temperature are bold. The rate constants obtained from the experiments with photolysis of N_2O are italicized.

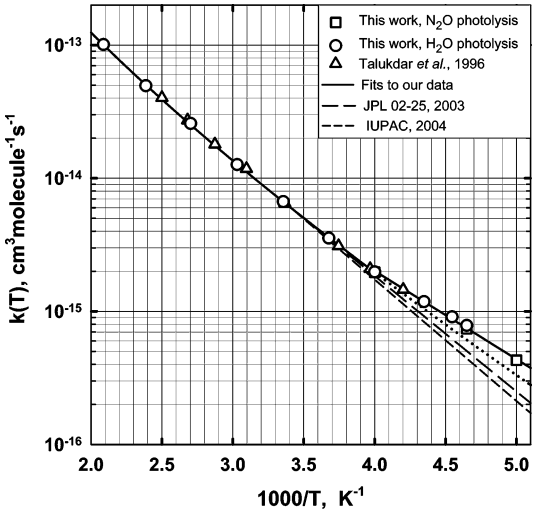

Figure 2. Arrhenius plot for the reaction of OH with H_2. (Symbol size exceeds the data uncertainties along both the ln k and $1/T$ axes.) The solid line represents eqs 15 and 16 for temperatures above and below 250 K, respectively. The dotted line is an extrapolation of eq 15 to lower temperatures. The dashed lines are NASA/JPL and IUPAC recommendations (T < 300 K).

The saturated water vapor pressure becomes too small at lower temperatures and, therefore, the reaction rate constant at T = 200 K was obtained using N_2O photolysis following the reaction between $O(^1D)$ and H_2 as the source of hydroxyl radicals.

$$N_2O + h\nu \rightarrow O(^1D) + N_2$$

$$O(^1D) + Ar, H_2, N_2O \rightarrow O(^3P) + Ar, H_2, N_2O$$

$$O(^1D) + H_2 \rightarrow OH + H$$

The saturated vapor pressure of water is still large enough at T = 250 K so that the test experiments with a wide range of H_2O concentrations (a factor of 30) could be performed at this

temperature. The precise value obtained in this set of experiments was compared with that obtained using N_2O as the photoprecursor. In contrast with the immediate formation of OH when H_2O is being photolyzed, this second source of OH involves the concurrence of chemical and quenching processes of $O(^1D)$ and, therefore, depends on the composition of the gas mixture in the reactor. It is thus more suitable at the lowest temperatures where higher concentrations of molecular hydrogen were used. Therefore, we consider our data obtained with H_2O as a precursor to be more accurate at $T = 250$ K and above.

To check the overall consistency of our results obtained with the different sources of OH, both of them were used for the measurements at $T = 250$ K. The experiments with the photolysis of water vapor to produce OH resulted in the rate constant of $k_{H_2}(250\ \text{K}) = (1.98 \pm 0.053) \times 10^{-15}$ cm^3 molecule^{-1} s^{-1}. Test experiments with various concentrations of H_2O, flash energies and total pressures were done to be confident in the thus-determined reaction rate constant.

In a second independent set of experiments N_2O was photolyzed to produce OH radicals in the reactor. Argon carrier gas was passing through the dry-ice-cooled trap ($T \cong 196$ K) to remove any traces of H_2O. In this case, no hydroxyl radicals could be detected in the absence of molecule hydrogen in the reactor. The temporal profile of the fluorescence signal (hydroxyl concentration), obtained in the experiment with the lowest concentration of molecular hydrogen, $I_{[H_2]_{min}}(t)$ was then used as a background to treat the data obtained at higher concentrations of hydrogen, $I_{[H_2]}(t)$ using our usual procedure.[31,34] Thus we obtained "incremental" decays due to reaction with H_2

$$\Delta\tau^{-1} = \frac{\partial}{\partial t}\ln\left\{\frac{I_{[H_2]_{min}}(t)}{I_{[H_2]}(t)}\right\} = k_{H_2}(T) \times \{[H_2] - [H_2]_{min}\} \quad (2)$$

and the reaction rate constant, $k_{H_2}(T)$ can be derived as a slope of the best linear fit to these data points:

$$k_{H_2}(T) = \frac{\partial\tau^{-1}}{\partial[H_2]} = \frac{\partial}{\partial[H_2]}\frac{\partial}{\partial t}\ln\left\{\frac{I_{[H_2]_{min}}(t)}{I_{[H_2]}(t)}\right\} \quad (3)$$

These expressions are similar to those we always used for the data treatment except the background decay, $I_{[H_2]_{min}}(t)$, is the measured decay of the fluorescence signal at the lowest molecular hydrogen concentration, not in the absence of the reactant. The fit to these data obtained at 4.00 kPa (30.0 Torr) total pressure resulted in $k_{H_2}^{N_2O}(250\ \text{K}) = (1.97 \pm 0.093) \times 10^{-15}$ cm^3 molecule^{-1} s^{-1}. These data were also treated using the background decay obtained in experiments at the same total pressure with the photolysis of H_2O. Such treatment of N_2O photolysis experiments resulted in $k_{H_2}^{N_2O/H_2O}(250\ \text{K}) = (2.00 \pm 0.054) \times 10^{-15}$ cm^3 molecule^{-1} s^{-1}. This is indicative of the absence of any additional background reactions of OH and complications in the experiments with N_2O photolysis. Thus, both experimental approaches with photolysis of H_2O and N_2O resulted in the same reaction rate constant at $T = 250$ K.

The same comparative experiments performed during two consecutive days at the lowest possible temperature, $T = 215$ K resulted in $k_{H_2}(215\ \text{K}) = (7.44 \pm 0.50) \times 10^{-16}$ cm^3 molecule^{-1} s^{-1}, $k_{H_2}^{N_2O}(215\ \text{K}) = (7.40 \pm 0.34) \times 10^{-16}$ cm^3 molecule^{-1} s^{-1}, and $k_{H_2}^{N_2O/H_2O}(215\ \text{K}) = (7.43 \pm 0.21) \times 10^{-16}$ cm^3 molecule^{-1} s^{-1}. There was no possibility to run additional test experiments at very different conditions at $T = 215$ K because the water partial pressure in the reactor was only about a half of the saturated vapor pressure at this temperature. For the same reason we are not as confident in the high accuracy of results obtained in H_2O photolysis experiments at 215 K as we are at higher temperatures. Nevertheless, a number of experiments with H_2O photolysis at 215 K were performed in the attempt to provide additional support to the data derived from N_2O photolysis experiments at this lowest temperature where both types of experiments are still possible. The fit to the combined data set from all experiments with photolysis of H_2O gives $k_{H_2}(215\ \text{K}) = (7.85 \pm 0.38) \times 10^{-16}$ cm^3 molecule^{-1} s^{-1}. The agreement between these results is quite satisfactory. Nevertheless, we decided to use the data obtained from N_2O photolysis experiments supported by the most recent experiments with H_2O photolysis to derive the recommendation for $k_{H_2}(215\ \text{K})$.

On the basis of the above, we can conclude that both experimental approaches with photolysis of H_2O and N_2O result in the same reaction rate constant within the statistical uncertainty of the measurements. Therefore, we assume that our experiments with N_2O photolysis at the lowest temperature, $T = 200$ K should be consistent with the data obtained over entire temperature range of the present study even though we could not employ tests using H_2O photolysis at this low temperature. The rate constant at $T = 200$ K was measured in two independent sets of experiments separated by two years and resulted in $k_{H_2}^{N_2O}(200\ \text{K}) = (4.38 \pm 0.24) \times 10^{-16}$ cm^3 molecule^{-1} s^{-1} *and* $k_{H_2}^{N_2O}(200\ \text{K}) = (4.31 \pm 0.30) \times 10^{-16}$ cm^3 molecule^{-1} s^{-1}, respectively.

Effect of OH Diffusion on the Measured Rate Constant. Any experimental procedure employed to measure the reaction rate constants using a pulse photolysis technique is based on the assumption that the background decay rate of OH (decay rate measured in the absence of the reactant under study) is independent of the presence of the reactant. In our experiments this background decay is assumed to be due to OH diffusion out of the viewing zone of the detection system. Moreover, in many cases the observed changes of decay rates due to reaction with H_2 are comparable with the background decay rates in our experiments. Therefore, the stability of the background decay rate is a necessary prerequisite for precise and accurate measurements of the rate constant. It becomes especially important in this case of studying the reaction of OH with hydrogen because diffusion of OH in the carrier gas, Ar, and in the reactant, H_2, is very different and high relative concentrations of H_2 are used in the experiments, especially at lower temperatures. Thus, the dilution of the carrier gas with hydrogen under the same total pressure will increase the "diffusional" decay in addition to the induced reaction decay that we are attempting to measure. This will result in systematic overestimation of the derived reaction rate constant. This systematic error can be more pronounced at lower total pressure and lower temperature experiments where larger relative concentrations of hydrogen are used.

To analyze for possible systematic error due to this change in OH diffusion rate, we can rewrite the main kinetic equation being used for the data treatment[31,34] more accurately to account for the change in OH diffusion:

$$k_{H_2}^{obs}(T) = \frac{1}{[H_2]}\frac{\partial}{\partial t}\ln\left\{\frac{I_0(t)}{I_{[H_2]}(t)}\right\} = \frac{1}{[H_2]}\frac{\partial}{\partial t}\ln\left\{\frac{I^0_{diff}(t)}{I^{[H_2]}_{diff}(t) \times \exp(-k_{H_2}[H_2] \times t)}\right\} = k_{H_2}(T) + \frac{1}{[H_2]}\frac{\partial}{\partial t}\ln\left\{\frac{I^0_{diff}(t)}{I^{[H_2]}_{diff}(t)}\right\} \quad (4)$$

Here $I^0_{diff}(t)$ and $I^{[H_2]}_{diff}(t)$ are the temporal profiles of the OH diffusional decay in the absence of the reactant ($[H_2] = 0$) and when H_2 is present in the mixture replacing an equivalent amount of carrier gas. In the case of experiments with high concentrations of hydrogen $I^0_{diff}(t)$ and $I^{[H_2]}_{diff}(t)$ may become different with the latter being a function of $[H_2]$ as mentioned above. One cannot obtain $I^{[H_2]}_{diff}(t)$ experimentally simply because the reaction with H_2 cannot be "switched off". Also, as discussed elsewhere,[31,34] the correct description and analysis of the diffusional decay of [OH] is actually impossible for a pulse experiment; even the functional form of the temporal profile of the ratio of interest, $I^0_{diff}(t)/I^{[H_2]}_{diff}(t)$ is unknown. However, we can measure the upper limits of this ratio directly in experiments performed at various pressures of the carrier gas to estimate the effect of the dilution with H_2 on results of our measurements. We recorded background decays at a number of slightly different pressures of the carrier gas in the vicinity of the "standard" total gas pressure used in the rate constant measurements. Such experiments were done around 16.5 Torr (13.5−18.5 Torr) at $T = 298$ K and around 30 Torr (26−36 Torr) at $T = 230$ K. Then, the decay obtained at the highest pressure in each set of experiments (which is supposed to be the slowest decay in each set) was used as a background decay to treat the rest of the data in the set. Our conventional point-by-point data treatment[31,34] was used to derive a decay rate, $\Delta\tau^{-1}_{\Delta[Ar]}$ due to a particular difference in the pressure (change of the carrier gas concentration $\Delta[Ar]$). Thus, we obtained the experimental dependences of changes of diffusional decay due to "dilution with vacuum", that is, with a "compound" that has an infinite coefficient of diffusion. The diffusion coefficient of OH in hydrogen is large but has a finite value. Therefore, these experimentally obtained values for $\Delta\tau^{-1}_{\Delta[Ar]}$ give us reasonable upper limits for the possible systematic overestimation of the rate constant due to dilution of carrier gas with hydrogen for any $\Delta[Ar] = [H_2]$

$$\Delta\tau^{-1}_{\Delta[Ar]} = \frac{1}{\Delta[Ar]}\frac{\partial}{\partial t}\ln\left\{\frac{I^0_{diff}(t)}{I^{\Delta[Ar]}_{diff}(t)}\right\} > \frac{1}{[H_2]}\frac{\partial}{\partial t}\ln\left\{\frac{I^0_{diff}(t)}{I^{[H_2]}_{diff}(t)}\right\} \quad (5)$$

These experiments indicate less than 0.7% possible error even at the lowest pressure, 16.5 Torr (2.2 kPa) at $T = 298$ K. The experiments at lower temperature $T = 230$ K and 30 Torr total pressure indicated less than 0.4−1% (from different experiments) possible error. Assuming the same changes in OH diffusion at $T = 200$ K, the possible overestimation of the rate constant will be less than 1−2%. Therefore, even at the highest relative concentrations of hydrogen in the reactor our experimental conditions and data treatment are quite adequate and do not cause any significant systematic error.

Reactive Impurity Check. The measured rate constant $k_{H_2}(T)$ is very small, particularly at lowest temperatures of this study. Therefore, the presence of reactive impurities in the sample of hydrogen could result in an overestimation of measured reaction rate constants and cause curvature of the Arrhenius plot. To avoid this possibility we used the highest purity hydrogen in all of our experiments (Spectra Gases Inc., 99.9999% stated purity with less than 0.1 ppm stated level total halocarbons impurity). To further check for the possible presence of reactive impurities from other occasional sources, we used different glass bulbs and different vacuum systems for the preparation and storage of the reactant mixtures to find no noticeable variation of the measured rate constant. In addition, two successive test experiments were done with this highest purity hydrogen sample and a sample from a different manufacturer with a very different stated purity (Matheson, 99.99% with less than ca. 0.8 ppm of total halocarbons impurity). Both experiments resulted in statistically indistinguishable reaction rate constants measured at the lowest temperature of this study: $k^{N_2O}_{H_2}(200\ K) = (4.31 \pm 0.46) \times 10^{-16}$ cm^3 molecule^{-1} s^{-1} and $k^{N_2O}_{H_2}(200\ K) = (3.92 \pm 0.44) \times 10^{-16}$ cm^3 molecule^{-1} s^{-1}, respectively. Additional spectral analysis of the hydrogen sample was performed to check the presence of possibly reactive impurities missed in the manufacturer's analysis. On the basis of reactivity toward OH and saturated vapor pressure at liquid nitrogen temperature, only ethylene, C_2H_4, could pose a real problem as a missing hydrocarbon microimpurity in hydrogen. Therefore, absorption of a hydrogen sample in the vacuum UV was checked between 160 and 180 nm where C_2H_4 has very strong and structured absorption spectrum.[35] The concentration of ethylene in the sample was estimated to be less than ca. 0.5 ppm. Although this upper limit well exceeds the manufacturer stated level of impurity, it could result in less than 3% overestimation of $k_{H_2}(200\ K)$. Given the purity of hydrogen used in all of our experiments and results of test experiments we can be confident that the obtained kinetic data are not affected by the reactions of OH with reactive impurities even at the lowest temperatures employed in this study.

Effect of "Secondary Chemistry". Secondary chemistry is a common source of a systematic error in the determination of OH reaction rate constants. Similar to the presence of reactive impurities, the appearance of "secondary chemistry" usually results in overestimating the reaction rate constant to be determined. To be confident in the precise and accurate value of the reaction rate constant to be reported, numerous test experiments were performed over the wide ranges of experimental parameters specified above. Generally speaking, the purpose of such experiments was to check the effects of the initial hydroxyl concentration (variation of water concentration and flash energy totaling in ca. 3 orders of magnitude in the expected range of $[OH]_0$), product accumulation in the reactor (variation of water concentration, flash energy, flash repetition rate, and the flow rate totaling in up to a factor of ca. 3×10^3 for the variation of the photoproducts accumulation rate) and the total pressure (a factor of 6). All of the results reported in this paper were obtained under conditions where the determined reaction rate constant depended on neither $[OH]_0$ nor the total pressure in the reactor. However, we could see such dependences at higher concentrations of H_2O in the mixture. At higher initial photolysis rate the measured rate coefficient exhibited a dependence on the flash energy, water concentration, and total pressure. It also showed a dependence on both the flash repetition rate and the total gas flow rate, that is, the residence time of the reacting mixture in the cell. These effects were more pronounced at lower temperatures and became less important at higher temperatures (see below). Test experiments performed at the total pressure 100 and 30 Torr at $T = 298$ K revealed no significant difference when helium was used as a carrier gas instead of argon. This confirms that the observed effects depend on the total pressure in the reactor and were not related to the rate of diffusion out of irradiated zone.

In this study of the reaction between OH and H_2, the chemistry in the reactor is simple and well quantified. However, a quantitative analysis of results of our test experiments is limited by the spatial distribution of reactants and their diffusion in the real time of the experiment. Nevertheless, we note that the only observed effect on the measured rate constant associated with these wide variations of experimental conditions was a

TABLE 2

reaction		$k_i(298) \times 10^{-12}$, $cm^3 molecule^{-1} s^{-1}$	E/R, K
$OH + H_2 \rightarrow H_2O + H$	(1)		
side products, HO_x formation:			
$OH + OH (+M) \rightarrow H_2O_2 (+M)$	(6)	2.2	"298/T"[a]
$OH + H_2O_2 \rightarrow H_2O + HO_2$	(7)	1.7	160
$HO_2 + HO_2 (+M) \rightarrow$ $H_2O_2 + O_2 (+M)$	(8)	1.9	−600
$OH + OH \rightarrow H_2O + O$	(9)	1.9	240
$OH + O \rightarrow H + O_2$	(10)	33	−120
$OH + HO_2 \rightarrow H_2O + O_2$	(11)	110	−250
hydroxyl regeneration:			
$H + HO_2 \rightarrow OH + OH$	(12)	81	0
$O + HO_2 \rightarrow OH + O_2$	(13)	59	−200

[a] $k_6(T) = k_6(298\ K) \times (298/T)$.

decrease in its value. Apparently, any "secondary chemistry" due to higher photolytic impact on the reaction mixture always resulted in regeneration of OH and, therefore, in an underestimation of the rate constant. Thus, "secondary chemistry" could not be responsible for the observed curvature of the Arrhenius plot at lower temperatures. Nevertheless, all reported rate constants were obtained under conditions where no secondary regeneration of OH could be discerned.

We can speculate on the chemical mechanism responsible for the apparent regeneration of hydroxyl radicals in this reaction mixture. In Table 2 we summarized fast reactions that could take place in our reactor along with the target reaction (100 Torr total pressure is assumed for reactions 6 and 8).

One can see that the increasing $[OH]_0$ (increasing H_2O concentration and/or flash energy), lowering temperature, and increasing the total pressure should promote the production of hydrogen peroxide. Increasing the flash repetition rate and decreasing the gas flow rate through the reactor should also promote accumulation of the stable product, H_2O_2, in any multiflash experiment. The presence of traces of H_2O_2 in the reactor can result in regeneration of OH primarily via reaction 12.

Discussion

On the basis of the precision of the results reported above and the established absence of any complications due to experimental artifacts, we believe that the accuracy of the rate constant for reaction 1 has been improved significantly in the present study as illustrated in Figure 1. Our results are in perfect agreement (within reported statistical uncertainties) with the latest published data[8] for this reaction at $T = 298$ K. Thus, we believe that the uncertainty of the recommended value for $k_{H_2}(T)$ can be decreased at room temperature.

Second, our study of reaction 1 has extended precise and accurate measurements of this rate constant to $T = 200$ K and revealed a noticeable curvature of the Arrhenius plot, which is indicative for some underestimation of the rate constant at lower temperatures by the current recommendations. At the extreme, these recommendations underestimate the rate constant at $T = 200$ K by a factor of 1.7 (NASA[9]) and 2.0 (IUPAC[10]), respectively. The deviation from a linear Arrhenius plot was probably present in the earlier studies by Smith and Zellner,[6] the only measurements performed at sufficiently low temperatures. Unfortunately, the lack of precision did not allow these authors to assign this curvature to anything other than secondary chemistry. The latest results reported by Talukdar et al.[8] are in excellent agreement with our data over the entire common temperature range between 238 and 400 K with the differences

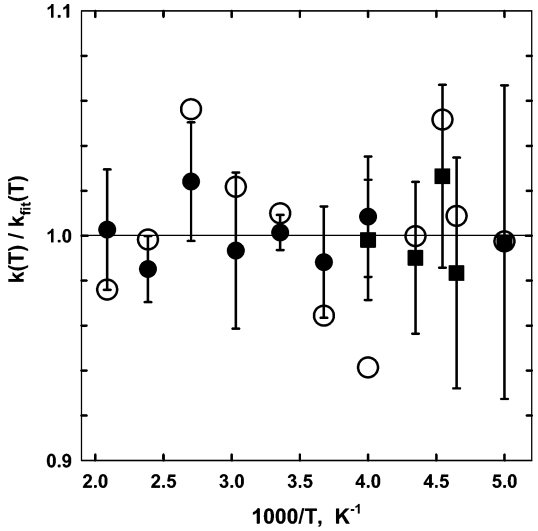

Figure 3. The measured rate constants normalized to the appropriate fit: eq 14, open circles; eq 15, filled circles; and eq 16, filled squares. Data points normalized to eqs 15 and 16 are shown with their normalized 2σ error bars.

not exceeding 5%. At their lowest temperature point ($T = 238$ K) the measured rate constant is already ca. 15% above that derived from the NASA-recommended Arrhenius dependence and could be indicative of curvature, although their measurements did not extend to sufficiently low temperature to confirm this behavior.

Data Presentation. A weighted fit of a modified Arrhenius expression to the bold highlighted data from Table 1 weighted by $(1/k_{H_2}(T))^2$ yields

$$k_{H_2}(T) = 7.483 \times 10^{-14} \times (T/298)^{3.861} \times \exp\{-723.4/T\}\ cm^3\ molecule^{-1}\ s^{-1} \quad (14)$$

which gives the rate constants that are within 6% of every data point. Although such differences might, at first glance, seem acceptable, this expression exhibits minor inconsistencies when residuals of the fit are analyzed. First, the residuals exhibit slightly nonuniform distribution. (These residuals are shown in Figure 3 as open circles.) Second, the formal application of the Chi Square test to the data with their corresponding statistical uncertainties results in a significantly large χ^2 value, which is indicative of possible inconsistency of the data with the chosen functional form. The analysis shows that the flattening of the Arrhenius plot at lower temperatures is the main reason for such inconsistency. However, limiting such a fit to data obtained between $T = 250$ K and $T = 479$ K yields

$$k_{H_2}(250-479\ K) = 4.27 \times 10^{-13} \times (T/298)^{2.406} \times \exp\{-1240/T\}\ cm^3\ molecule^{-1}\ s^{-1} \quad (15)$$

which fits the data considerably better and does not exhibit these inconsistencies. This dependence is drawn in Figure 2, and residuals of the fit are shown in Figure 3 as filled circles. The extrapolation of this dependence (eq 15) to the lower temperatures (shown as a dotted line in Figure 2) results in an increasing underestimation of the rate constant (up to ca. 30% at $T = 200$ K).

The data between 200 and 250 K can be separately fit to a simple Arrhenius expression yielding

$$k_{H_2}(200-250\ \mathrm{K}) = 9.01 \times 10^{-13} \times \exp\{-(1526 \pm 70)/T\}\ \mathrm{cm^3\ molecule^{-1}\ s^{-1}} \quad (16)$$

This dependence is also shown in Figure 2 and residuals of the fit are shown in Figure 3 as filled squares. Thus, the combination of eqs 15 and 16 is the best presentation of our data over the entire temperature range. The data reported by Talukdar et al.[8] are within 4% of those given by these equations.

Both the NASA[9] and IUPAC[10] Data Evaluation groups use a common two-parameter Arrhenius expression in their evaluation of k_i(298 K) and E/R. However, because of noticeable curvature of the derived Arrhenius dependence for $k_{H_2}(T)$, such approximation will introduce small but statistically significant biases to the predicted rate constant.

The rate constant at $T = 298$ K was derived from the most intensive set of measurements and test experiments to be

$$k_{H_2}(298\ \mathrm{K}) = (6.67 \pm 0.08) \times 10^{-15}\ \mathrm{cm^3\ molecule^{-1}\ s^{-1}}\ \text{with}\ f_{H_2}(298\ \mathrm{K}) = 1.038 \quad (17)$$

where the uncertainty factor f_{H_2}(298 K) represents the 95% confidence limit derived from the sum of the (2σ) statistical standard error reported in Table 1 and estimated systematic uncertainty of 3%. This factor allows k_{H_2}(298 K) to span the interval of $(6.42-6.92) \times 10^{-15}$ cm^3 molecule^{-1} s^{-1}, which overlaps all of the previously reported results within their reported statistical uncertainties. This uncertainty factor increases to $f_{H_2}(200\ \mathrm{K}) = 1.13$. Thus, following the formulation of the NASA Panel for Data Evaluation[9] the uncertainty factor for room temperature and below can be presented as

$$f_{H_2}(T) = 1.04 \times \exp\left\{50 \times \left|\frac{1}{T} - \frac{1}{298}\right|\right\} \quad (18)$$

One should note however, that the $f_i(T)$ factors appearing in the NASA Evaluation must be squared to yield similar 95% confidence limits.

A simple Arrhenius fit of our data below $T = 300$ K results in

$$k_{H_2}(T < 300\ \mathrm{K}) = 1.48 \times 10^{-12} \times \exp\{-(1635 \pm 83)/T\},\ \mathrm{cm^3\ molecule^{-1}\ s^{-1}} \quad (19)$$

which gives $k_{H_2}(298\ \mathrm{K}) = (6.14 \pm 0.52) \times 10^{-15}$ cm^3 molecule^{-1} s^{-1}, 9% below our reported value. Fixing k_{H_2}(298 K) to the measured value a revised simple Arrhenius fit yields

$$k_{H_2}(T < 300\ \mathrm{K}) = 2.05 \times 10^{-12} \times \exp\{-(1707 \pm 53)/T\},\ \mathrm{cm^3\ molecule^{-1}\ s^{-1}} \quad (20)$$

However, because of curvature in the Arrhenius plot this expression overestimates the rate constant by ca. 7% at the atmospherically important temperature $T = 272$ K while it underestimates k_{H_2}(200 K) by ca. 8%. Although these errors are small, a better representation of the data at atmospherically relevant temperatures is given by the combination of eqs 15 and 16.

Atmospheric Implications. The atmospheric lifetime of H_2 and its global atmospheric removal rate due to the reaction with hydroxyl radicals can be estimated by using the well-known approach of Prather and Spivakovsky[36] as the following

$$\tau^{OH}_{H_2} = \frac{k_{MCF}(272\ \mathrm{K})}{k_{H_2}(272\ \mathrm{K})}\,\tau^{OH}_{MCF} = 10.0\ \text{years} \quad (21)$$

where $\tau^{OH}_{H_2}$ and $\tau^{OH}_{MCF} = 5.99$ years[34] are the lifetimes of H_2 and methyl chloroform, respectively, due to reactions with hydroxyl radicals in the troposphere only, and $k_{H_2}(272\ \mathrm{K}) = 3.59 \times 10^{-15}$ cm^3 molecule^{-1} s^{-1} (eq 15) and $k_{MCF}(272\ \mathrm{K}) = 6.0 \times 10^{-15}$ cm^3 molecule^{-1} s^{-1} (ref 9) are the rate constants for the reaction of OH with hydrogen and methyl chloroform at $T = 272$ K.[33] Strictly speaking, eq 21 gives the lifetime due to reaction with OH in the troposphere only.[36] The additional stratospheric burden of the compound should be considered along with the additional sink due to its reaction with OH in the stratosphere. To a first approximation, these two corrections offset and eq 21 yields a good approximation of the global atmospheric lifetime.[31,34] Assuming the uniform distribution of H_2 over the entire atmosphere and accepting its average concentration of 0.53 ppmv,[1] we can also estimate the total amount of H_2 in the entire atmosphere as ca. 187 MT and the rate of H_2 removal from the entire atmosphere by the reaction with OH to be ca. 19 MT/year. Note that soil uptake is considered to be the dominant sink of H_2 from the troposphere with the estimated removal rate of ca. 56 MT/year.

Acknowledgment. This work was supported by the Upper Atmosphere Research Program of the National Aeronautics and Space Administration. We thank Dr. Robert Huie for fruitful discussions and Dr. Larissa Martynova for her assistance in some test experiments.

References and Notes

(1) Novelli, P. C.; Lang, P. M.; Masarie, K. A.; Hurst, D. F.; Myer, R.; Elkins, J. W. *J. Geophys. Res.* **1999**, *104*, 30427−30444.
(2) Tromp, T. K.; Shia, R.-L.; Allen, M.; Eiler, J. M.; Yung Y. L. *Science* **2003**, *300*, 1740−1742.
(3) Warwick, N. J.; Bekki, S.; Nisbet, E. G.; Pyle, J. A. *Geophys. Res. Lett.* **2004**, *31*, L05107.
(4) Prather, M. *Science* **2003**, *302*, 581−582.
(5) Schultz, M. G.; Diehl, T.; Brasseur, G. P.; Zittel, W. *Science* **2003**, *302*, 624−627.
(6) Smith, I. W. M.; Zellner, R. *J. Chem. Soc., Faraday Trans. 2* **1974**, *70*, 1045−1056.
(7) Ravishankara, A. R.; Nicovich, J. M.; Thompson, R. L.; Tully, F. P. *J. Phys. Chem.* **1981**, *85*, 2498−2503.
(8) Talukdar, R. K.; Gierczak, T.; Goldfarb, L.; Rudich, Y.; Rao, B. S. M.; Ravishankara, A. R. *J. Phys. Chem.* **1996**, *100*, 3037−3043.
(9) Sander, S. P.; Friedl, R. R.; Golden, D. M.; Kurylo, M. J.; Huie, R. E.; Orkin, V. L.; Moortgat, G. K.; Ravishankara, A. R.; Kolb, C. E.; Molina, M. J.; Finlayson-Pitts, B. J. *Chemical Kinetics and Photochemical Data for Use in Atmospheric Studies, Evaluation No. 14*; JPL Publication 02-25; Jet Propulsion Laboratory, California Institute of Technology: Pasadena, CA 2003.
(10) Atkinson, R.; Baulch, D. L.; Cox, R. A.; Crowley, J. N.; Hampson, R. F.; Hynes R. G.; Rossi, M. J.; Troe, J. *Atmos. Chem. Phys.* **2004**, *4*, 1461−1738.
(11) Chakraborty, A.; Truhlar, D. G. *Proc. Natl. Acad. Sci. U.S.A.* **2005**, *102*, 6744−6749.
(12) Goldfield, E. M.; Gray, S. K. *J. Chem. Phys*. **2002**, *117*, 1604−1613.
(13) Manthe, U.; Matzkies. F. *J. Chem. Phys.* **2000**, *113*, 5725−5731.
(14) Troya, D.; Lakin, M. J.; Schatz, G. C.; Gonzalez, M. *J. Chem. Phys.* **2001**, *115*, 1828−1842.
(15) Smith, I. W. M.; Crim, F. F. *Phys. Chem. Chem. Phys.* **2002**, *4*, 3542−3551.
(16) Kaufman, F.; Del Greco, F. P. *Symp. Int. Combust. Proc.* **1963**, *9*, 659.
(17) Dixon-Lewis, G.; Wilson, W. E.; Westenberg, A. A. *J. Chem. Phys.* **1966**, *44*, 2877−2884.
(18) Greiner, N. R. *J. Chem. Phys.* **1967**, *46*, 2795−2799.
(19) Greiner, N. R. *J. Chem. Phys.* **1969**, *51*, 5049−5051.
(20) Dodonov, A. F.; Lavrovskaya, G. K.; Tal'roze, V. L. *Kinet. Catal.* **1969**, *10*, 573−579.
(21) Stuhl, F.; Niki, H. *J. Chem. Phys.* **1972**, *57*, 3671−3677.

(22) Westenberg, A. A.; DeHaas, N. *J. Chem. Phys.* **1973**, *58*, 4061.

(23) Overend, R. P.; Paraskevopoulos, G.; Cvetanovic, R. J. *Can. J. Chem.* **1975**, *53*, 3374−3382.

(24) Atkinson, R.; Hansen, D. A.; Pitts, J. N., Jr. *J. Chem. Phys.* **1975**, *62*, 3284−3288.

(25) Biermann, H. W.; Zetzsch, C.; Stuhl, F. *Ber. Bunsen-Ges. Phys. Chem.* **1978**, *82*, 633−639.

(26) Tully, F. P.; Ravishankara, A. R. *J. Phys. Chem.* **1980**, *84*, 3126.

(27) Zellner, R., Steinert, W. *Chem. Phys. Lett.* **1981**, *81*, 568−572.

(28) Schmidt, V.; Zhu, G.-Y.; Becker, K. H.; Fink, E. H. *Phys. Chem. Behav. Atmos. Pollut. Proc. Eur. Symp.* **1984**, 177−187.

(29) Certain commercial equipment, instruments, or materials are identified in this article in order to adequately specify the experimental procedure. Such identification does not imply recognition or endorsement by the National Institute of Standards and Technology nor does it imply that the material or equipment identified are necessarily the best available for the purpose.

(30) Kurylo, M. J.; Cornett, K. D.; Murphy, J. L. *J. Geophys. Res.* **1982**, *87*, 3081−3085.

(31) Orkin, V. L.; Huie, R. E.; Kurylo, M. J. *J. Phys. Chem.* **1996**, *100*, 8907−8912.

(32) Orkin, V. L.; Khamaganov, V. G.; Guschin, A. G.; Huie, R. E.; Kurylo, M. J. *J. Phys. Chem.* **1997**, *101*, 174−178.

(33) Spivakovsky, C. M.; Logan, J. A.; Montzka, S. A.; Balkanski, Y. J.; Foreman-Fowler, M.; Jones, D. B. A.; Horowitz, L. W.; Fusco, A. C.; Brenninkmeijer, C. A. M.; Prather, M. J.; Wofsy, S. C.; McElroy, M. B *J. Geophys. Res.* **2000**, *105*, 8931−8980.

(34) Kurylo, M. J.; Orkin, V. L. *Chem. Rev.* **2003**, *103*, 5049−5076.

(35) Orkin, V. L.; Huie, R. E.; Kurylo, M. J. *J. Phys. Chem.* **1997**, *101*, 9118−9124.

(36) Prather, M.; Spivakovsky, C. M. *J. Geophys. Res.* **1990**, *95*, 18723−18729.